



# COB-2021-0598 MODELING, SIMULATION AND CONTROL OF QUADROTOR FOR TRANSPORTATION OF A LOAD SUSPENDED BY A CABLE

**Gabriel Gomes Passos**

**Yohan Ali Diaz Mendez**

Universidade Federal de Itajubá (UNIFEI)

gabrielgpassos@unifei.edu.br

yohan.g8@unifei.edu.br

**Abstract.** *Unmanned Aerial Vehicles (UAV) have been used in several applications such as monitoring and security missions, filming and photography, mapping and pulverization in agricultural areas and, particularly, load transportation. This last application presents itself as a very useful and efficient alternative for military operations, delivering packages and civil constructions. Quadrotors, more specifically, have gained notoriety in recent years due to the relative simplicity of their dynamics, their low cost of research and production when compared to other vehicles, in addition to their vast operational capacity. Its ability to take off and land vertically, hover and its high maneuverability guarantee the ability to follow any 3D trajectory, reaching target positions that traditional aircraft are not capable of. The transport of slung loads suspended by cables presents advantages over grasping the load to the drone structure for this type of operation, however the presence of the load introduces great instabilities to the drone during the flight. For that reason, it is necessary to carry out research in this area, detailing the design and implementation of control techniques to stabilize the load and control the trajectory of the drone. Therefore, the main objective of this work is to implement a control strategy that allows a quadrotor to transport a slung load to a target position quickly, precisely and with good damping of oscillations. To reach this objective, a nonlinear 3D model of the system dynamics, composed of the quadrotor and the load suspended by a rigid cable, is developed using the Euler-Lagrange method. Based on this model, the controller is developed using the Universal Integrative Regulator nonlinear control technique, based on sliding mode control with the addition of a conditional integrator (CISMC). Moreover, a classic PID controller is tuned to control the same system in order to obtain a reference to assess the benefits of the CISMC controller. The validation of both the model and the compared controllers are done through numerical simulations via MATLAB/Simulink. In the present work, it is expected to obtain positive results of performance and stability of the system, achieving shorter response times and less oscillations when the nonlinear controller is applied. It is expected, with the CISMC technique, to eliminate or at least overcome the inherent instability problems of the studied system, which classical control techniques cannot handle.*

**Keywords:** *quadrotor, slung load, non linear control, Universal Integral Regulator, PID controller.*

## 1. INTRODUCTION

A quadrotor presents great advantages when compared to other existing vehicles. Its ability to take-off and land vertically allows it to perform these manoeuvres in reduced space areas, expanding considerably its operational capacity. Moreover, its ability to hover and move in any direction makes it capable of following any 3D trajectory within a good time interval. The relative simplicity of its flight dynamics, combined with the low cost of research and production when compared to other aircraft has boosted the use of quadrotors in recent years (Cutler, 2012). As a result, its applicability in the most diverse branches of society is extensive, especially, on carrying out missions of mapping, monitoring, filming and photography, security, civil construction, among others.

Among the many interesting applications of quadrotors, load transportation stands out. Delivery operations, transport of supplies to restricted access regions, assistance in civil constructions and transport of military cargo are just a few examples that justify the high potential of UAVs for this type of applications nowadays, due to the significant advantages when compared to conventional means of load transportation. Quadrotors can perform tracking missions quickly, allowing them to carry out transport and delivery tasks autonomously, safely and efficiently. On the other hand, the effect of the interaction between the drone and the load directly influences the dynamics of the system, making it even more unstable and complex (Ortiz, 2017).

Due to the mentioned applicability of quadrotors for load transportation previously given, research in this field has become quite typical in recent years. Traditionally, it was done with helicopters (Stuckey, 2001) but, more recently, it has been done in quadrotors, two main approaches have been followed. The first one, followed in Mellinger *et al.* (2013), consists of grasping the load close to the centre of gravity, which presents some limitations, being one of them, the increase

in mass and rotational inertia caused by the attached load which will slow down the attitude dynamics and response of the drone. Additionally, the drone is not able to deliver the payload if the landing area is inaccessible. Finally, in case the load be too heavy or too big to be attached directly to the drone frame, its transportation will not be possible. In Praveen (2015) and Sreecath *et al.* (2013), the load is hung by a cable. Following this second approach, not only the load can be delivered without the drone landing, but also the drone preserves its agility. There is even the possibility of using several drones cooperating between them to transport heavier loads in Pizetta *et al.* (2016) and Mellinger *et al.* (2013).

The introduction of the hanging load by a cable increases both the modelling and the controlling complexity. Classic linear control techniques, such as Linear Quadratic Regulator (LQR) (Akyazi *et al.*, 2012) and PID control (Sudha and Deepa, 2014) are common approaches applied to UAV control. However, in more complex nonlinear systems, such as the one studied in this work, these techniques may not satisfy the desirable performance requirements for their application (Sousa, 2013).

First works aimed at controlling the drone without considering the load. The forces and moments exerted by the load on the drone are considered as disturbances that the controller needs to deal with robustly (Palunko *et al.*, 2012).

In Ortiz *et al.* (2017), the classical PID control strategy is implemented on a quadrotor in which no sensor is employed to estimate the orientation of the cable nor the load's position. The tuning of the controller is done in order to satisfy mixed  $H_\infty$  and pole placement requirements. The author obtained noticeable improvements when modelling the motor-propeller as a nonlinear model instead of using the usual first order model. To begin with, the author uses a time constant which is different when the motors demand increases than when it is lowered. Additionally, the static gain is quadratic with the pulse duration, instead of being constant.

In Pizetta *et al.* (2015), a geometric nonlinear control system using feedback linearization is used to asymptotically stabilize the position of the vehicle and keep the cable in its vertical position. The effects of the load are considered as a modelled disturbance applied to the system and the goal is not the load guidance.

In Nicotra *et al.* (2014), a new control law is proposed in order to an aerial robot to track a desired reference while simultaneously limiting the sway of the payload. This law is based on the idea of nested saturation. The stability of the approach is proven rigorously by means of ISS arguments.

In Potter *et al.* (2011), the load oscillations are damped by pre-filtering the reference of the UAV using input shaping.

In Palunko *et al.* (2012) the authors present two different approaches. The first one uses feedback linearization in a model without the swinging mass and compensating the effects of the load oscillation with adaptive control. The second approach is based on the idea of generating swing free trajectories recurring to dynamic programming.

In Goodarzi *et al.* (2014) and Goodarzi (2016), the cable is considered flexible, being modelled as a system of serially-connected links. A geometric nonlinear control system is presented to asymptotically stabilize the position of the quadrotor while aligning the links to the vertical direction. Proof of mathematical stability was given using the Lyapunov theory.

As referred previously, using multiple drones to carry out a cooperative transporting mission could be very interesting. In this field, Maza *et al.* (2010) presents the control system for the transportation of a slung load by means of one or several helicopters. In Goodarzi and Lee (2015), an arbitrary number of quadrotors is used in order to transport a rigid body. The goal is to stabilize each drone, maintaining its cable vertical. However, this is only possible to do without the drones colliding if the load is big enough. And in Pizetta *et al.* (2016) a controller for two UAVs carrying a suspended load is proposed. When the cable is taught, it is represented as a highly rigid spring. Fictitious repulsion forces between the UAVs are introduced in order to prevent them from colliding with each other.

In the literature, it is possible to find both linear and non-linear control laws used as solutions for UAV stability and guidance problems. Sliding Mode Control (SMC) is a nonlinear control technique widely known for its robustness against disturbances, uncertain parameters and in cases where the complete dynamics is not considered or known in the model, being widely used in research related to UAVs, which are characterised as dynamically unstable nonlinear systems in various conditions (Herrera *et al.*, 2015). However, when aerodynamic effects are considered, the SMC presents a static error in steady state, since its structure is modeled as a sliding surface with proportional-derivative action, as shown by Labbadi *et al.* (2018). In the present work, the authors makes use of an improvement of the SMC technique, adding an integrative action to the SMC control, obtaining satisfactory results in terms of performance and robustness in a tracking problem of a quadrotor.

The addition of an integrative action to the SMC control, by means of a conventional integrator, produces a degradation of the system transient response. In Seshagiri and Khalil (2005), it was proposed the use of integrative action only under certain conditions, eliminating performance degradation in transient regime, using a control law called Conditional Integrator Sliding Mode Control (CISMC), or Universal Integrative Regulator. In Mendez (2018), the author uses an CISMC controller in a quadrotor to solve a tracking problem and proves the stability of the system through the Lyapunov principle. In the present work, the CISMC is used in order to solve tracking problems in quadrotors with slung loads being the main novelty of the paper.

## 2. PROBLEM STATEMENT

Although the CISMIC has proven effective and superior in many aspects (performance, robustness, etc.) when compared to traditional control techniques (Mendez, 2018), few studies were directed to the application of this technique in control problems with quadrotors, and studies on the application of this technique in systems related to cargo transport with UAVs were not found in the literature.

Therefore, this work aims to develop a controller capable of stabilising the oscillations of a pendular load attached to a quadrotor through a cable. The CISMIC non-linear control technique is used, based on sliding mode control with the addition of a conditional integrator.

In order to reach the objective, a deduction of a high-level 3D model of the system is necessary. This model is then used to develop the controllers. The model should be as general as possible, so that after validation it becomes a useful tool for designing and validating controllers for load carrying purposes with varying configurations.

After the development of the controller using the CISMIC technique, it is pre-validated in a numerical simulator implemented in MATLAB®/Simulink®. Finally, the results are compared with the responses of the same system controlled by a PID controller, a classical linear control approach.

## 3. DYNAMIC MODEL OF THE SYSTEM

To design the desired controller, a model of the system composed of the quadrotor, the cable and the load must be deduced. This section presents the general aspects of the modeled quadrotor, its configuration, reference axis system, model assumptions, pendular load dynamics and, finally, deduction of the equations using the Euler-Lagrange method.

### 3.1 Modelling of the Quadrotor

For the dynamic model of the drone, a quadrotor in “X” configuration is considered. This type of UAV has four rotors, two at the front and two at the back, whose rotation directions must be defined so that opposite motors rotate in the same direction. The configuration of the quadrotor, as well as the motors rotation directions, are shown in Fig. 1.

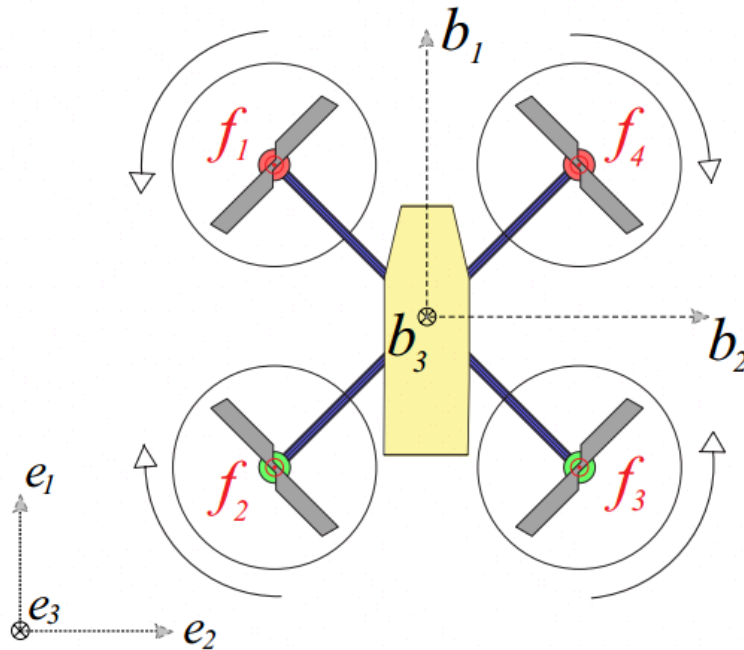


Figure 1. Schematic representation of motors configuration.

The vectors  $e_1$ ,  $e_2$  and  $e_3$  define the three axes ( $x, y, z$ ) representing the inertial frame, whereas the vectors  $b_1$ ,  $b_2$  and  $b_3$  define the axes representing the body frame. The inertial frame can be obtained from the body frame applying to it a series of three rotations of angles  $\phi$ ,  $\theta$  and  $\psi$ , respectively about the  $x$ ,  $y$  and  $z$  axes. If  $\mathbf{R}_x(\phi)$ ,  $\mathbf{R}_y(\theta)$  and  $\mathbf{R}_z(\psi)$  represent the rotations of a frame about its  $x$ ,  $y$  and  $z$  axis respectively, then the matrix representing the transformation of the body frame to the inertial frame is  $\mathbf{R}(\phi, \theta, \psi) = \mathbf{R}_z(\psi)\mathbf{R}_y(\theta)\mathbf{R}_x(\phi)$ , which can be written as follows:

$$\mathbf{R} = \begin{bmatrix} c_\theta c_\psi & c_\psi s_\theta s_\phi - s_\psi c_\phi & c_\psi s_\theta c_\phi + s_\psi s_\phi \\ c_\theta s_\psi & s_\psi s_\theta s_\phi + c_\psi c_\phi & s_\psi s_\theta c_\phi - c_\psi s_\phi \\ -s_\theta & s_\phi c_\theta & c_\phi c_\theta \end{bmatrix}, \quad (1)$$

with  $c_x$  and  $s_x$  standing for  $\cos x$  and  $\sin x$  respectively. A point in space whose coordinates  $\{a_b \ b_b \ c_b\}^T$  are constant in the body frame has coordinates  $\{a_e \ b_e \ c_e\}^T = \mathbf{R}(\phi, \theta, \psi)\{a_b \ b_b \ c_b\}^T$  in the inertial frame. The matrix that allows to transform the rate of change of the Euler angles into the angular velocity written in the body fixed frame is  $\mathbf{W}(\phi, \theta)$ . This matrix is such that  $\boldsymbol{\omega}^b = \{p \ q \ r\}^T = \mathbf{W}(\phi, \theta)\{\dot{\phi} \ \dot{\theta} \ \dot{\psi}\}^T$ , and it can be written as follows:

$$\mathbf{W}(\phi, \theta) = \begin{bmatrix} 1 & 0 & -\sin \theta \\ 0 & \cos \phi & \cos \theta \sin \phi \\ 0 & -\sin \phi & \cos \phi \cos \theta \end{bmatrix}, \quad (2)$$

Each of the quadrotor's engines can generate a thrust of  $\mathbf{f}_i \in \mathbb{R}^3$ ,  $i \in \{1, 2, 3, 4\}$ . In the body frame, these forces are all aligned with the z-axis. The movement of each engine also generates a moment about the z-body-axis. Therefore, through the combination of the four engine thrusts, it is possible to generate a force aligned with the z-body-axis, as well as a moment about any of the three body-axis.

### 3.2 Model Assumptions and Definition of Variables

To model the system, the following assumptions have been made:

- The load is a point mass;
- The cable connecting the load and the quadrotor has no mass nor inertia and it is rigid of constant length;
- The suspension point is frictionless and located at the drone centre of gravity (CG);
- The aerodynamic drag forces are neglected;
- The effect of the air flow caused by the quadrotor on the load is neglected;
- The drone is symmetrical in relation to all the axes of the body, meaning its inertia matrix  $\mathcal{I}$  is diagonal;
- The drone is rigid, and flapping effects are therefore neglected.

Using the three first assumptions, the load can be considered as a spherical pendulum connected to a frictionless joint. The fact that the cable's length is constant implies that if the position of the joint where the cable is hung is known, then the load's position can be written in spherical coordinates, through two angles  $\alpha$  and  $\beta$ , and a radius corresponding to the length of the cable,  $l$ . This is developed in section 3.3

The influence of the load is seen by the drone through the traction force that the drone needs to exert on the cable to sustain the load. The force is always aligned with the cable, so it changes both in module and direction in time.

Due to the second assumption, this model does not consider the flexibility of the cable, nor the possibility of it being slack and the tension applied being zero. Consequently, some flight modes are not considered by the model and the domain of validity and utilisation of both the model and the developed controller is restricted. The model should not be considered valid in any situation where the cable becomes slack or bends. Such is the case during:

- Take-off.
- Landing.
- Rapid descents.
- Aggressive manoeuvres.

Additionally, the model is not valid for high speed operation, since the drag forces acting both on the quadrotor and the cable become non-negligible. The model used in this work can be considered valid whenever the cable is taut and operating speeds are not high.

The variables used in the model deduction are:

- $\mathbf{x}_Q = \{x_Q \ y_Q \ z_Q\}^T \in \mathbb{R}^3$  : coordinates defining the position of the quadrotor in the inertial frame;
- $\mathbf{x}_L = \{x_L \ y_L \ z_L\}^T \in \mathbb{R}^3$  : coordinates defining the position of the load in the inertial frame;
- $l$  : length of the cable;
- $m_Q$  : mass of the quadrotor;
- $m_L$  : mass of the load;

- $\mathcal{I} = \text{diag}(I_{xx}, I_{yy}, I_{zz})$  : inertia matrix of the quadrotor;
- $\phi$  : roll angle of the quadrotor;
- $\theta$  : pitch angle of the quadrotor;
- $\psi$  : yaw angle of the quadrotor;
- $\alpha$  and  $\beta$  : angles defining the load's position with respect to the point where the cable is hung in the drone;
- $\omega = \{p \ q \ r\}^T$  : angular velocity of the drone in its body frame;
- $\mathbf{R}(\phi, \theta, \psi)$  : matrix transforming the body frame into the inertial frame;
- $\mathbf{W}(\phi, \theta)$  : matrix transforming the rate of change of the Euler angles into the angular velocity written in the body fixed frame;
- $\mathcal{L}$  : Lagrangian;
- $T$  : kinetic energy of the system;
- $V$  : potential energy of the system;
- $\mathbf{q}$  : generalised coordinates of the system.

### 3.3 Load Kinematics

As a result of considering the cable's length ( $l$ ) constant, knowing the position where the cable is hung allows determining the position of the load in terms of two swing angles,  $\alpha$  and  $\beta$ , in spherical coordinates. These two angles, which define the cable's orientation, are presented in Fig. 2.

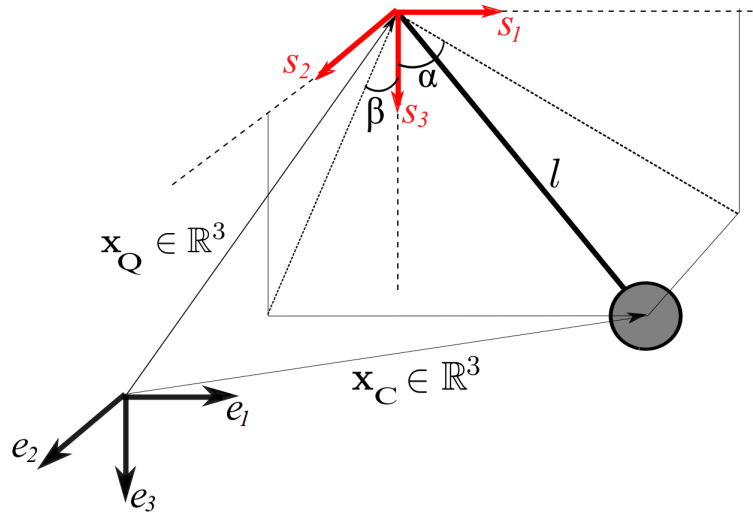


Figure 2. Angles defining the position of the load.

The vectors  $\mathbf{s}_1$ ,  $\mathbf{s}_2$  and  $\mathbf{s}_3$  are parallel to  $\mathbf{e}_1$ ,  $\mathbf{e}_2$  and  $\mathbf{e}_3$  respectively and placed in the joint where the cable is hung. Departing from a configuration where the cable is coincident with  $\mathbf{s}_3$ , any cable orientation can be obtained through a rotation of  $\beta$  about  $\mathbf{s}_1$  (this rotation sets  $y_L$ ), followed by a rotation of  $\alpha$  about  $\mathbf{s}_2$  (this rotation sets  $x_L$  and  $z_L$ ).

The equation that describes these rotations and relate the position of the quadrotor and the position of the load through the orientation of the cable ( $\alpha, \beta$ ) can be written as follows:

$$\begin{Bmatrix} x_L \\ y_L \\ z_L \end{Bmatrix} = \begin{Bmatrix} x_Q \\ y_Q \\ z_Q \end{Bmatrix} + \begin{Bmatrix} l \cos \beta \sin \alpha \\ l \sin \beta \\ l \cos \beta \cos \alpha \end{Bmatrix}, \quad (3)$$

As a result of the assumptions and modelling choices made, the generalised coordinates of the system are:

$$\mathbf{q} = \{x_Q \ y_Q \ z_Q \ \int p \ \int q \ \int r \ \alpha \ \beta\}^T, \quad (4)$$

In addition to the 6 degrees of freedom that are usually used to define the quadrotor's position and attitude, the two swing angles  $\alpha$  and  $\beta$  consist of new degrees of freedom of the system. Since the inputs of the system are the same as when there is no load (forces and moments generated by the drone), the two new degrees of freedom are non-actuated.

Once the relation between the quadrotor's and the load's positions has been determined, it is possible to obtain the Jacobian matrix  $\mathbf{J}(\mathbf{q})$ , which represents the transformation of the generalised coordinates derivatives  $\dot{\mathbf{q}}$  into the velocities of the system, as follows:

$$\mathbf{J} = \begin{bmatrix} 1 & 0 & 0 & 0 & 0 & 0 & 0 & 0 & 0 \\ 0 & 1 & 0 & 0 & 0 & 0 & 0 & 0 & 0 \\ 0 & 0 & 1 & 0 & 0 & 0 & 0 & 0 & 0 \\ 0 & 0 & 0 & 1 & 0 & 0 & 0 & 0 & 0 \\ 0 & 0 & 0 & 0 & 1 & 0 & 0 & 0 & 0 \\ 0 & 0 & 0 & 0 & 0 & 1 & 0 & 0 & 0 \\ 1 & 0 & 0 & 0 & 0 & 0 & l \cos \alpha \cos \beta & -l \sin \alpha \sin \beta & 0 \\ 0 & 1 & 0 & 0 & 0 & 0 & 0 & l \cos \beta & 0 \\ 0 & 0 & 1 & 0 & 0 & 0 & -l \sin \alpha \cos \beta & -l \cos \alpha \sin \beta & 0 \\ 0 & 0 & 0 & 0 & 0 & 0 & 1 & 0 & 0 \\ 0 & 0 & 0 & 0 & 0 & 0 & 0 & 1 & 0 \end{bmatrix}, \quad (5)$$

### 3.4 Model Synthesis: Euler-Lagrange Equations

When there is no load, but only the drone, it is quite common to follow the Newtonian approach to obtain the equations modelling the system's dynamics. However, when there is a load, the projections required by the Newtonian approach become very complex. As a result, the Lagrangian approach is in this case preferred.

The Euler-Lagrange equations are given by:

$$\frac{d}{dt} \left[ \frac{\partial \mathcal{L}}{\partial \dot{\mathbf{q}}} \right] - \frac{\partial \mathcal{L}}{\partial \mathbf{q}} = \mathbf{f}_{\text{ext}}, \quad (6)$$

where the Lagrangian is given by:

$$\mathcal{L}(\dot{\mathbf{q}}, \mathbf{q}) = T(\dot{\mathbf{q}}, \mathbf{q}) - V(\mathbf{q}), \quad (7)$$

where  $T$  is the kinetic energy of the system, expressed in terms of the generalised coordinates  $\mathbf{q}$  and its derivatives  $\dot{\mathbf{q}}$ ,  $V$  is the potential energy of the system and  $\mathbf{f}_{\text{ext}}$  is the control inputs of the system.

The translational component of the kinetic energy is given by the sum of the translational kinetic energies of the drone and the load (Eq. 8). Similarly, the rotational component is obtained by summing the kinetic rotational energies of the drone and the load (Eq. 9), considering  $I_L = I_{Lxx} = I_{Lyy}$ . However, the fact of the load being considered as a point mass in the model implies that it has no inertia ( $I_L = 0$ ) and therefore does not contribute to the rotational energy of the system.

$$T_{\text{trans}} = T_{\text{trans}_Q} + T_{\text{trans}_L} = \frac{1}{2} m_Q (\dot{x}_Q^2 + \dot{y}_Q^2 + \dot{z}_Q^2) + \frac{1}{2} m_L (\dot{x}_L^2 + \dot{y}_L^2 + \dot{z}_L^2), \quad (8)$$

$$T_{\text{rot}} = T_{\text{rot}_Q} + T_{\text{rot}_L} = \frac{1}{2} (I_{xx} \omega_x^2 + I_{yy} \omega_y^2 + I_{zz} \omega_z^2) + \frac{1}{2} I_C (\alpha^2 + \beta^2), \quad (9)$$

Finally, defining  $\mathbf{M}_s = \text{diag}(\mathbf{M}_Q, \mathbf{M}_L, \mathcal{I})$  as the matrix of masses and inertias of the system, the total kinetic energy  $T$  is written in a convenient way as follows:

$$T(\dot{\mathbf{q}}, \mathbf{q}) = T_{\text{trans}} + T_{\text{rot}} = \frac{1}{2} \dot{\mathbf{q}}^T \mathbf{J}(\mathbf{q})^T \mathbf{M}_s \mathbf{J}(\mathbf{q}) \dot{\mathbf{q}}, \quad (10)$$

As far as the potential energy is concerned, it can be written simply as:

$$V(\mathbf{q}) = -m_Q g z_Q - m_L g (z_Q + l \cos \alpha \cos \beta), \quad (11)$$

The external control inputs of the system  $\mathbf{f}_{\text{ext}}$  are expressed by Eq. 12. The external force  $\mathbf{f} = \mathbf{R}\{0 \ 0 \ f\}^T$  is defined in the inertial coordinate system as a result of the lift force generated by the motors. The external torque  $\boldsymbol{\tau} = \{\tau_\phi \ \tau_\theta \ \tau_\psi\}^T$  is defined in the body coordinate system, with  $\tau_\phi$ ,  $\tau_\theta$  and  $\tau_\psi$  being the moments generated by the combined motors forces in relation to  $\mathbf{b}_1$ ,  $\mathbf{b}_2$  and  $\mathbf{b}_3$ , respectively.

$$\mathbf{f}_{\text{ext}} = \{\mathbf{f}^T \ \boldsymbol{\tau}^T \ 0 \ 0\}^T, \quad (12)$$

Thus, the system dynamics equations can finally be obtained through Eq. 6. The resulting equations are quite complex and, therefore, it would not be possible to present them in this work.

The quadrotor dynamics can be rewritten in the input affine form  $\dot{\mathbf{X}} = f(\mathbf{X}) + g(\mathbf{X})\mathbf{u}$  by doing the change of variables  $\mathbf{X} = \{x_Q, y_Q, z_Q, \phi, \theta, \psi, \alpha, \beta, \dot{x}_Q, \dot{y}_Q, \dot{z}_Q, p, q, r, \dot{\alpha}, \dot{\beta}\}^T$  where  $\mathbf{X}$  is the state vector  $\mathbf{X} \in \mathbb{R}^{16}$ .

#### 4. SYNTHESIS OF THE CONTROLLERS

The model described in section 3 is used to design two different controllers. The first one is a PID controller, to be used as a reference based on a classical linear control approach. The second one is a CISM (Conditional Integrator Sliding Mode Control, also known as Universal Integral Regulator), a nonlinear control technique based on sliding mode control with the addition of an integrative action under certain conditions, which will be described below, according to the study developed in Mendez (2018).

The basic control structure is a cascade control loop. The inner loop consists of the attitude controller, which controls the input moments for the system so that the quadrotor reaches a certain attitude angle, but this is not the focus of this work. The outer loop consists of the position controller, which generates both the attitude reference angles for the drone to reach a certain location in the  $xy$ -plane and the lift force necessary for the drone to reach a certain altitude. Considering this, the controllers were designed for position control in  $x$ ,  $y$  and  $z$  coordinates.

##### 4.1 PID controller

The PID control approach is characterised as a feedback control technique with the objective of minimising the error of a given output of the controlled system and can be described as follows:

$$u_i = K_P^i e^i + K_I^i \int e^i dt + K_D^i \frac{d}{dt} e^i, \quad (13)$$

where  $e^i$  and  $u^i$  are, respectively, the tracking error and the control input for the  $i$ -th output.  $K_P$ ,  $K_I$  and  $K_D$  are constant gains to be chosen.

For the altitude controller, a simple PID controller according to Eq. 13 was proposed. For  $x$  and  $y$  controllers, however, it is proposed to add a feedback control component with respect to angles  $\alpha$  and  $\beta$ , which define the position of the load in relation to the drone. The presence of the load introduces many instabilities in the system, so that a simple PID controller may not be able to simultaneously control the system with good performance and good disturbance rejection, in order to reduce load oscillations. Thus, for the  $xy$  position, the designed control action is defined as in Eq. 14.

$$\begin{cases} u_x = K_P^x e^x + K_I^x \int e^x dt + K_D^x \dot{e}^x - K_\alpha \alpha - K_{\dot{\alpha}} \dot{\alpha}, \\ u_y = K_P^y e^y + K_I^y \int e^y dt + K_D^y \dot{e}^y - K_\beta \beta - K_{\dot{\beta}} \dot{\beta}, \end{cases} \quad (14)$$

where  $K_\alpha$ ,  $K_{\dot{\alpha}}$ ,  $K_\beta$  and  $K_{\dot{\beta}}$  are constant gains to be chosen.

##### 4.2 CISM controller

According to Seshagiri and Khalil (2005), the sliding surface of the CISM is defined as in Eq. 15.

$$s_i = k_0^i \sigma_i + \sum_{j=1}^{\rho_i-1} k_j^i e_j^i + e_{\rho_i}^i, \quad (15)$$

where  $e_j^i$  is the tracking error for the  $i$ -th output,  $\rho$  is the relative degree of the system and  $k_1^i, \dots, k_{\rho_i-1}^i$  are positive constants to be chosen. The  $\sigma_i$  state is the output of the conditional integrator defined in Eq. 16.

$$\dot{\sigma}_i = -k_0^i \sigma_i + \mu_i \text{sat}(s_i/\mu_i), \quad (16)$$

with  $k_0^i$  and  $\mu_i$  positive parameters.

Finally, the CISM control law  $u$  is defined in Eq. 17, as a result of the continuous approximation of an ideal SMC given by  $v_i$ .

$$\begin{cases} u_i = g(e^i, \dot{e}^i)^{-1} [-f(e^i, \dot{e}^i) + v_i], \\ v_i = -K_i \text{sat}(s_i/\mu_i), \end{cases} \quad (17)$$

The position controller has three system outputs, states  $x, y$ , and  $z$ , and three control inputs,  $\phi_{des}$ ,  $\theta_{des}$  and  $f_{des}$ , where  $f_{des}$  is an actual control input of the system and  $\phi_{des}$  and  $\theta_{des}$  are the desired Euler angles for the attitude controller. The control objective consists of designing independent SISO CISM controllers in order to track a reference altitude and a desired trajectory in the  $xy$  plane.

For the altitude controller, it is easy to obtain a direct relation between the output  $\ddot{z}_Q$  and  $f$  from the dynamic equations of the model, which implies two important conclusions. The first one is that, for the pair  $\ddot{z}_Q \rightarrow f$ , it is possible to see that the relative degree of the altitude controller is  $\rho = 2$ , since only two derivatives of the output are needed to get a direct

relation with the input. The second conclusion is that the load dynamics can easily be considered for the controller design, as the functions  $f(x)$  and  $g(x)$  are made explicit. However, due to the fact that they are very long, they are not presented here.

On the other hand, for the  $x$  and  $y$  controllers, obtaining a direct relationship between the  $x$  and  $y$  outputs and the  $\phi$  and  $\theta$  attitude angles becomes a very complex task when considering the load dynamics. For this reason, for the design of these controllers, the load is considered as a disturbance to the system and, therefore, the dynamic equations of the model are simplified by making  $m_L = \alpha = \dot{\alpha} = \beta = \dot{\beta} = 0$ . Thus, it is possible to define  $u_x = (\cos\phi\cos\psi\sin\theta + \sin\phi\sin\psi)$  and  $u_y = (\cos\phi\sin\psi\sin\theta - \sin\phi\cos\psi)$  as virtual control inputs, which must be inverted to obtain the euler angle commands (Eq. 18) that will be used as a reference for the attitude controller.

$$\begin{cases} \phi_{des} = \arcsin(u_x \sin\psi - u_y \cos\psi), \\ \theta_{des} = \arcsin\left(\frac{u_x \cos\psi + u_y \sin\psi}{\cos\phi_{des}}\right), \end{cases} \quad (18)$$

Therefore, according to Eq. 19, the control inputs for the position controller can be written as follows:

$$\begin{cases} u_x = \frac{m}{f_{des}} [-K_x \text{sat}(s_x/\mu_x)], \\ u_y = \frac{m}{f_{des}} [-K_y \text{sat}(s_y/\mu_y)], \\ f_{des} = g(e^z, \dot{e}^z)^{-1} [-f(e^z, \dot{e}^z) - K_z \text{sat}(s_z/\mu_z)], \end{cases} \quad (19)$$

## 5. SIMULATION TESTS AND DISCUSSION

This section presents the numerical simulation results for the controller to demonstrate the performance and robustness of the proposed CISMIC control technique when compared to a classical PID control strategy. The parameters of the quadrotor used in the simulation are presented in Tab. 1 and the parameters of both the CISMIC and PID controller are presented in Tab. 2.

Table 1. System parameters.

Parameter	Value	Parameter	Value
$g$ [m/s <sup>2</sup> ]	9.81	$I_{xx}$ [kg·m <sup>2</sup> ]	0.0018
$m_Q$ [kg]	0.500	$I_{yy}$ [kg·m <sup>2</sup> ]	0.0018
$m_L$ [kg]	0.100	$I_{zz}$ [kg·m <sup>2</sup> ]	0.0033
$l$ [m]	1.0		

Table 2. Control parameters.

CISMIC	Value	PID	Value
$k_0^x, k_1^x, K_x, \mu_x$	0.1, 0.5, 40, 30	$K_P^x, K_I^x, K_D^x, K_\alpha, K_{\dot{\alpha}}$	0.25, 0.015, 0.3, 0.15, 0.05
$k_0^y, k_1^y, K_y, \mu_y$	0.1, 0.5, 40, 30	$K_P^y, K_I^y, K_D^y, K_\beta, K_{\dot{\beta}}$	0.25, 0.015, 0.3, 0.15, 0.05
$k_0^z, k_1^z, K_z, \mu_z$	1, 1.5, 5, 0.15	$K_P^z, K_I^z, K_D^z$	2.06, 0.6, 2.1

The proposed control method has been tested by solving the position tracking problem presented in Fig. 3, which shows the trajectory of both the drone and the load for each of the controllers. The initial position and euler angle values of the quadrotor for simulation tests are respectively  $\{0, 0, 0\}$ m and  $\{0, 0, 0\}$ rad, and the initial angle values for the load are  $\{\alpha, \beta\} = \{0, 0\}$ rad.

As presented in Mendez (2018), two performance index are used to quantify the compared performance of both controllers, a performance index to the accumulated error ( $AE$ ) defined as  $AE^i = \sum_{t=0}^{t=T} |e_1^i|$  and other to measure the control demand  $CD^i = \sum_{t=0}^{t=T} |u_p|$  for  $i = x, y, z$  along the simulation time  $T$ .

Figure 4 presents the altitude response of the system during the simulation. As expected, the CISMIC performed better than the PID control, converging in a shorter response time without any overshoot. The  $AE$  index confirms this conclusion, with  $AE_{CISMIC}^z = 0.6021$  and  $AE_{PID}^z = 1.347$ , showing that the CISMIC presented a more precise result. In terms of control demand, the performance indices were  $CD_{CISMIC}^z = 294.3$  and  $CD_{PID}^z = 294.4$ , indicating a similar performance between the two controllers. However, it is possible to notice in the graph that the CISMIC proved to be more robust to the perturbations generated by the steps in  $x$  and  $y$ , since the PID controller presented small oscillations in the control demand signal.

Figure 5 presents the response of the system related to the  $x$ -position. The designed CISMIC controller resulted in a lower overshoot and faster steady-state error reduction, although it achieved a slower transient response and the load

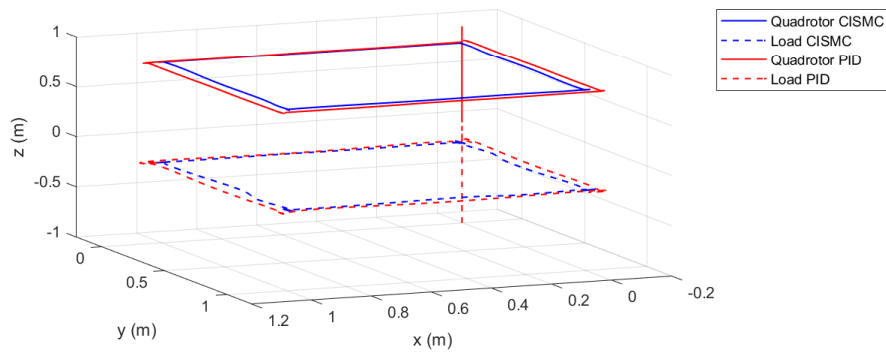


Figure 3. 3D trajectory.

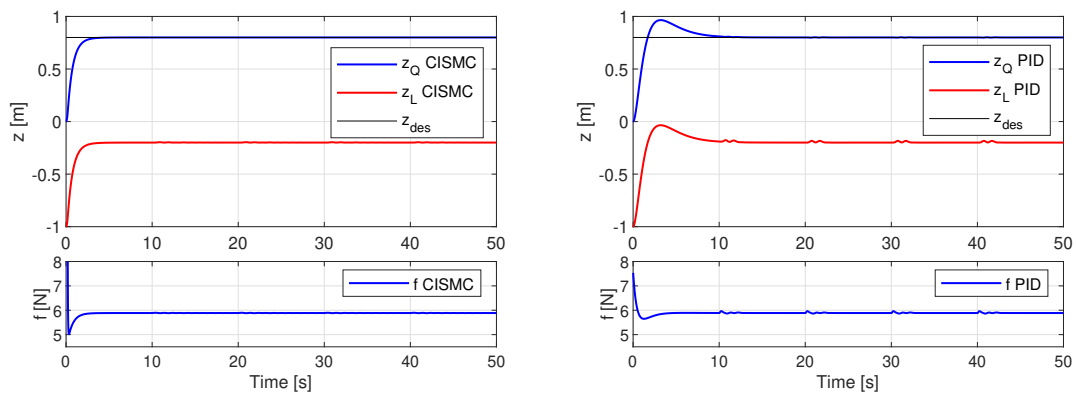


Figure 4. z-position system response.

oscillated longer when compared to the PID controller results. The  $AE$  index also indicates that, with  $AE_{CISMIC}^x = 4.002$  and  $AE_{PID}^x = 3.575$ . However, it is worth remembering that the CISMIC does not consider the existence of the load in its design, while the PID controller has a feedback of the load angles and angular velocities, showing a good robustness of the CISMIC. In terms of control demand, the performance indices were  $CD_{CISMIC}^x = 0.00386$  and  $CD_{PID}^x = 0.01643$ , indicating a much superior performance of the CISMIC, which can also be graphically observed through the lower attitude angle and torque demanded.

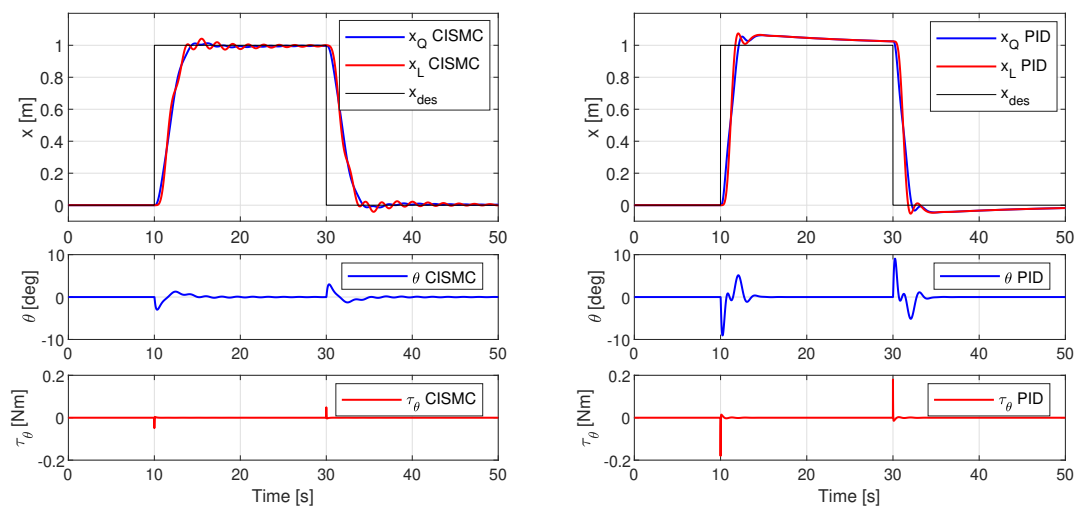


Figure 5. x-position system response.

The responses of the system in x and y positions are very similar, since it was assumed that the drone presents the same inertia with respect to x and y axes, for which reason only the response of the system in x-position is presented.

## 6. CONCLUSION

In the present work, it was designed and analysed a Conditional Integrator Sliding Mode Control (CISMC) approach applied to a highly unstable system composed of a quadrotor and a load suspended by a cable, whose dynamic model was deduced. The results of a PID controller, a classic linear control technique, and the new non-linear controller developed were compared. The proposed control approach was validated through simulations, proving to be a sufficiently robust method with good performance to follow the trajectory proposed in the presented tracking problem.

## 7. REFERENCES

- Akyazi, O., Usta, M.A. and Akpınar, A.S.A., 2012. "A self-tuning fuzzy logic controller for aircraft roll control system". *International Journal of Control Science and Engineering*, Vol. 2, No. 6, pp. 181–188.
- Cutler, M.J., 2012. *Design and control of an autonomous variable-pitch quadrotor helicopter*. Master's thesis, Massachusetts Institute of Technology, Cambridge, USA.
- Goodarzi, F.A., 2016. "Autonomous aerial payload delivery with quadrotor using varying length cable". *IEEE International Conference on Advanced Mechatronic Systems*.
- Goodarzi, F.A., Lee, D. and Lee, T., 2014. "Geometric stabilization of a quadrotor uav with a payload connected by flexible cable". *American Control Conference*.
- Goodarzi, F.A. and Lee, T., 2015. "Stabilization of a rigid body payload with multiple cooperative quadrotors". *Journal of Dynamic Systems Measurement and Control*.
- Herrera, M., Chamorro, W. and Gómez, A.P., 2015. "Sliding mode control: An approach to control a quadrotor". *Asia-Pacific Conference on Computer Aided System Engineering*, pp. 314–319.
- Labbadi, M., Cherkaoui, M. and Guisser, M., 2018. "Modeling and robust integral sliding mode control for a quadrotor unmanned aerial vehicle". *International Renewable and Sustainable Energy Conference*, pp. 1–16.
- Maza, I., Bernard, M., Kondak, K. and Ollero, A., 2010. "Multi-uav cooperation and control for load transportation and deployment". *Journal of Intelligent and Robotic Systems*, Vol. 57, pp. 417–449.
- Mellinger, D., Shomin, M., Michael, N. and Kumar, V., 2013. "Cooperative grasping and transport using multiple quadrotors". In *Distributed Autonomous Robotic Systems*. Vol. 83, pp. 545–558.
- Mendez, Y.A.L., 2018. *Estudo detalhado do regulador integrativo universal e comparação com outras técnicas de controle*. Ph.D. thesis, Universidade Federal de Itajubá, Itajubá, Brasil.
- Nicotra, M., Garone, E., Naldi, R. and Marconi, L., 2014. "Nested saturation control of an uav carrying a suspended load". *American Control Conference (ACC)*.
- Ortiz, N.A.S., 2017. *Analyse de la robustesse de la loi de commande d'un quadrirotor embarquant une charge suspendue par un câble (in Français)*. Master's thesis, Institut National des Sciences Appliquées, Estrasburgo, Francia.
- Ortiz, N.A.S., Laroche, E., Kiefer, R. and Durand, S., 2017. "Controller tuning strategy for quadrotor mav carrying a cable-suspended load". *International Micro Air Vehicle Conference and Flight Competition (IMAV)*.
- Palunko, I., Cruz, P. and Fierro, R., 2012. "Agile load transportation: safe and efficient load manipulation with aerial robots". *IEEE Robotics Automation Magazine*, Vol. 19, No. 3, pp. 69–79.
- Pizetta, I.H.B., Brandão, A.S. and Sarcinelli, M., 2015. "Modelling and control of a pvtol quadrotor carrying a suspended load". *International Conference on Unmanned Aircraft Systems (ICUAS)*.
- Pizetta, I.H.B., Brandão, A.S. and Sarcinelli, M., 2016. "Cooperative quadrotors carrying a suspended load". *International Conference on Unmanned Aircraft Systems (ICUAS)*.
- Potter, J., Singhose, W. and Costello, M., 2011. "Reducing swing of model helicopter sling load using input shaping". *IEEE International Conference on Control and Automation (ICCA)*.
- Praveen, R.K.J., 2015. "Transportation of cable suspended load using unmanned aerial vehicles". *Delft University of Technology, MSC Thesis*.
- Seshagiri, S. and Khalil, H.K., 2005. "Robust output feedback regulation of minimum-phase nonlinear systems using conditional integrators". *Automatica*, Vol. 41, No. 1, pp. 43–54.
- Sousa, M.S., 2013. *Modelagem, simulação e controle não linear de aviões muito flexíveis*. Ph.D. thesis, Instituto Tecnológico Aeronáutica, São José dos Campos, Brasil.
- Sreecath, K., Michael, N. and Kumar, V., 2013. "Trajectory generation and control of a quadrotor with a cable-suspended load - a differentially flat hybrid system". *IEEE International Conference on Robotics and Automation*, pp. 4888–4895.
- Stuckey, R.A., 2001. "Mathematical modelling of helicopter slung-load systems". *Commonwealth of Australia*, , No. 12.
- Sudha, G. and Deepa, S.N., 2014. "Optimization for pid control parameters on pitch control of aircraft dynamics based on tuning methods". *Applied Mathematics Information Sciences*, Vol. 10, No. 1, p. 343.

## 8. RESPONSIBILITY NOTICE

The authors are solely responsible for the printed material included in this paper.